High Thermal Conductivity of Single Polyethylene Chains Using Molecular Dynamics Simulations

Asegun Henry and Gang Chen
Department of Mechanical Engineering, Massachusetts Institute of Technology, 77 Massachusetts Avenue, Cambridge, Massachusetts 02139, USA
(Received 2 June 2008; published 5 December 2008)

We use molecular dynamics simulations to calculate the thermal conductivity of single polyethylene chains employing both the Green-Kubo approach and a modal decomposition method. Although bulk polyethylene is a thermal insulator, our results suggest that the thermal conductivity of an individual polymer chain can be very high, even divergent in some cases. Our results suggest that polymers can be engineered with high thermal conductivity for a wide variety of applications.

DOI: 10.1103/PhysRevLett.101.235502 PACS numbers: 63.22.−m, 63.20.D−, 63.20.kg, 66.70.Hk

Bulk polymer materials are generally regarded as thermal insulators because they have low thermal conductivities on the order of 0.1 W/m K. An individual polymer chain, however, may have extremely high thermal conductivity. This hypothesis is built on the observations of Fermi, Pasta, and Ulam [1] as well as decades of discussion on anomalous heat conduction in one-dimensional lattices [2–4]. Many of these previous works, however, were based on simplified models. To our knowledge, the most realistic thermal simulation of a polymer chain was that of Freeman, Morgan, and Cullen [5], but the inherent boundary scattering in their nonequilibrium approach would have concealed any potentially nonattenuating modes or divergent (infinite) thermal conductivity (TC). Experimentally [6], 2 orders of magnitude increase in thermal conductivity has been reported by stretching bulk samples of polyethylene (PE) to increase the alignment of the constituent chains. In this Letter, we explored the limiting thermal conductivity of individual PE chains and found that they have very high thermal conductivity, which could tend to infinity, under certain conditions. Our results are intended to stimulate further research into the development of high thermal conductivity polymer materials.

In this Letter, we carried out molecular dynamics simulations of single PE chains using the Green-Kubo approach as well as a modal analysis technique [7–9] to determine phonon relaxation times. Because our simulations used periodic boundary conditions, the trajectories reflected the dynamics of a finite set of modes that were allowed to propagate on an infinite chain, uninhibited by boundaries. This means that the total number of modes in each simulation was limited by the corresponding number of unit cells (ucs) in the simulation domain. Unlike nonequilibrium methods [5], however, theses modes were allowed to propagate indefinitely and were only attenuated by phonon-phonon interactions. This approach was chosen so that boundary scattering would not conceal any divergent behavior. Based on the relaxation times extracted from these simulations, we estimated the TC of finite length chains suspended between two contacts. The results showed that the TC can exceed 100 W/m K (5×10^{-10} W/K conductance) if the chain is longer than 40 nm. Our Green-Kubo results agreed with these calculations and even showed divergent (TC $\rightarrow \infty$) behavior when the simulation domain was longer than 40 ucs ($\sim$10 nm). Further testing and analysis suggested that this divergence was not a result of unphysical numerical artifacts. Our analysis shows that the phenomenon may be related to low frequency modes that do not fully attenuate, similar to the behaviors observed in other previous works [2–4] that used simplified models.

The molecular dynamics simulations were conducted using the LAMMPS software package [10], which was developed at Sandia National Laboratories. All simulations employed periodic boundary conditions, used a 0.25 femtosecond time step, and were carried out at equilibrium in the microcanonical ensemble (total energy variations less than 0.0001%) for 10 nanoseconds, with 100 picoseconds of equilibration time. The initial conditions for all simulations used the equilibrium (minimum energy) positions of the zigzag conformation and random velocities corresponding to a quantum-corrected temperature $T = 300$ K, based on the following semiclassical definition [11,12]: $E_{\mathrm{MD}} = \sum_p \sum_k h\nu[\exp(h\nu/k_B T) - 1]^{-1}$. E_{MD} is the total energy of the molecular dynamics initial condition, p and k denote the polarizations and wave vectors, respectively, h is Planck's constant, k_B is Boltzmann's constant, and ν is the phonon frequency. This definition matches the total vibration energy in the molecular dynamics (classical) system with that of a corresponding quantum system of phonons at 300 K. As other authors have noted [11,12], this correction is necessary for more accurate results and comparison with experiments and is particularly important for this investigation, because the phonon frequencies span more than 2 orders of magnitude. For this system the quantum-corrected temperature 300 K corresponds to $\sim$85 K if we employ the equipartition-based temperature definition, which is more widely used. Although the results presented in this Letter were run at the quantum-corrected 300 K, we also ran additional simulations at 300 K using

the more traditional equipartition temperature definition. These simulations exhibited similar behaviors with even higher thermal conductivity, stronger divergence, and stronger normal mode correlation effects, which are discussed later.

The adaptive intermolecular reactive bond order (AIREBO) potential [13], which is based on the widely used second-generation Brenner potential [14], was employed to describe the atomic interactions. In contrast to the simplified toy models of earlier works [1,5], where anharmonicity was not based on chemical bonding considerations, AIREBO has anharmonicity built in through its empirical modeling of hydrocarbon bonding. Although AIREBO was mostly tested against the structural and thermodynamic properties of condensed phase hydrocarbons [13], the Brenner potential, which comprises the covalent portion of AIREBO, has shown good agreement with experiments on the thermal conductivity of diamond [15]. In contrast to Freeman, Morgan, and Cullen's [5] use of the Kirkwood model [16] for PE, which lumps the repeating CH_2 units together as a single mass, our use of AIREBO includes each hydrogen atom explicitly. By allowing hydrogen atom vibrations, the AIREBO model provides a more realistic description of the anharmonicity, as hydrogen atom displacements can affect the forces between neighboring carbon atoms through 3-body and 4-body angular terms. Our use of a more realistic anharmonic model could allow the higher frequency (30–60 THz) modes to scatter the low frequency nonattenuating modes observed in earlier works [1–4].

To determine the limiting TC of an infinitely long chain we used the Green-Kubo method [7,9,12], where the TC is given by $\kappa = Vk_B^{-1}T^{-2}\int_0^\infty \langle Q_z(t)Q_z(t+t')\rangle dt'$. In this expression, TC is calculated by integrating the heat flux autocorrelation (HFAC) function $\langle Q_z(t)Q_z(t+t')\rangle$, where z denotes the component of the heat flux directed along the carbon backbone of the chain, V is the chain's volume, and T is the temperature. For systems with one-dimensional symmetry, such as a single PE chain, defining the volume becomes somewhat arbitrary. In this Letter, we have taken the volume as the length of the simulation domain multiplied by an 18 Å^2 cross-sectional area, which is based on the unit cell dimensions of PE's idealized bulk lattice structure. Here we emphasize that our reported TC values could be scaled by a different choice of cross-sectional area, and therefore the corresponding conductance values are provided where appropriate. Additional details pertaining to the calculation procedure can be found in previous work by Henry and Chen [7] and the derivation of the heat flux operator has been presented by Hardy [17].

One limitation of the Green-Kubo approach is that the analysis of one chain cannot be used to predict the TC of other chains with different lengths. To predict the TC of PE chains larger than what we are currently able to simulate directly, we used a modal analysis approach to determine the phonon relaxation times [7–9]. Using this approach, which is based on the Boltzmann transport equation (BTE) and relaxation time approximation, we can determine the PE chain TC from $\kappa = V^{-1}\sum_p \sum_k Cv^2\tau$. In this expression, which we will refer to as the BTE-TC expression, C is the specific heat per mode, v is the phonon group velocity, and τ is the relaxation time, which is obtained from the normal mode autocorrelation (NMAC) function, as proposed by Ladd, Moran, and Hoover [8]. The NMAC is based on the temporal fluctuations of the mode's total energy, which are calculated from a modal decomposition of the atomic trajectory [7,9]. Further details on the modal decomposition methodology and prerequisite lattice dynamics calculations have been thoroughly discussed elsewhere [7]. All other necessary details pertaining to the calculation procedures can be found in previous works that employ these approaches [7,9].

Our calculation of the phonon dispersion for a single PE chain is shown in Fig. 1 (solid lines) along with the Kirkwood model used by Freeman, Morgan, and Cullen (dashed lines), with arrows denoting the two transverse acoustic polarizations (labeled 1 and 2), the longitudinal acoustic polarization (labeled 3), and the torsional acoustic branch (labeled 4) [18]. When compared to experimental data and *ab initio* calculations of the phonon dispersion for bulk PE [19], AIREBO shows good agreement with the phonon frequencies. Our dispersion also shows similar groups of phonon branches, which serve as further indication that AIREBO is well suited for description of PE's vibrational/phonon dynamics. The Kirkwood model, on the other hand, underestimates the acoustic mode frequencies, which would lead to lower group velocities.

The cumulative HFAC integration from several simulations is shown in Fig. 2, where the time axis represents the

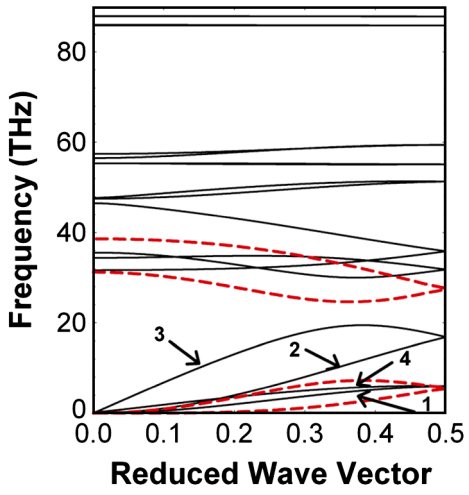

FIG. 1 (color online). Phonon dispersion for a single PE chain, calculated from the AIREBO potential [13] used in this work and the Kirkwood model [16], used in previous works [5,22]. For the AIREBO model there are a total of 18 phonon branches (2 branches ~56 THz and 4 branches between 80–90 THz). Numbers identify the two transverse (1 and 2), longitudinal (3), and torsional (4) acoustic polarizations [18].

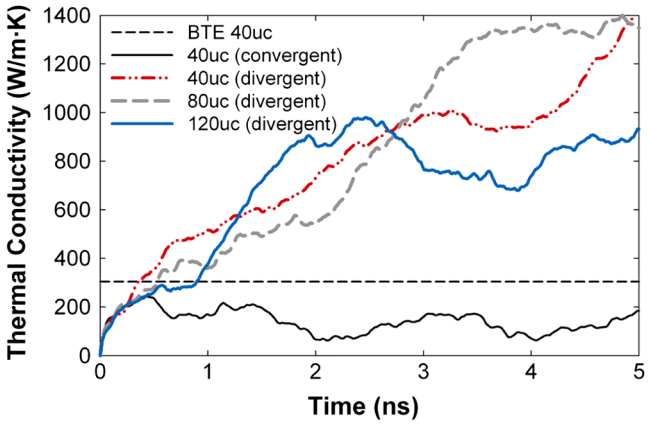

FIG. 2 (color online). Green-Kubo thermal conductivity integrals for different simulation domain sizes. One convergent and one divergent case are shown for the 40 uc simulations, as well as divergent cases for the 80 and 120 uc simulations. The BTE 40 uc line indicates the thermal conductivity computed from the BTE-TC expression, when contributions from the two nonattenuating modes are neglected.

increasing integration limit of the Green-Kubo integral. In other reports [7,12] where three-dimensional bulk inorganic crystalline materials were studied with the Green-Kubo method, the integration of HFAC functions typically converged within the first 500 picoseconds. Here, however, we extended the integration to 5 nanoseconds, because we noticed that in certain cases, the HFAC integral continued increasing.

More than 60 simulations with different initial random velocities were run with varying domain sizes. The results in Fig. 2 are examples from each domain size that clearly exhibited contrasting behavior. Many other cases in between these extremes were also observed, but examination of these results indicated that the degree of divergence changes with initial conditions. Figure 2 shows two very different behaviors for the 40 uc domain, and the line labeled BTE 40 uc shows the TC calculated for a 40 uc chain using the BTE-TC expression. The same type of converging/diverging behavior and its dependence on the initial condition was also observed for simulation domains longer than 40 ucs. Divergence was not observed in shorter chains, and we were unable to clearly identify any specific aspect of the initial condition that directly caused the divergence. We believe the behavior is likely due to some feature of the trajectory as opposed to solely being attributed to the random initial velocities.

This type of diverging behavior has also been observed in previous studies with simplified models [1–4]. The major difference here is that we used a more realistic model and expected the strongly embedded anharmonicity and inclusion of hydrogen atoms to discourage such behavior in our simulations. To test whether or not the phenomenon was due to numerical artifacts or physically meaningful aspects of the model, we recomputed the trajectory of several divergent cases using the same initial conditions but changed several atomic masses to that of heavier isotopes [2]. This physically meaningful modification introduced enough isotope scattering that the previously divergent HFAC integrals converged (not shown). This indicated that the divergent phenomenon was likely due to some nonlinear feature of the model.

To further investigate this phenomenon, we examined each mode's NMAC in the 40 uc case and noticed that almost all of the modes exhibited decaying behavior. The longest wavelength modes of the polarizations labeled 1 and 4 in Fig. 1 displayed distinctly different behavior. The NMAC functions for this transverse acoustic and torsional acoustic mode, shown in Fig. 3, remained correlated after 5 nanoseconds, which suggests that these modes do not completely attenuate. The strong self-correlation in these NMACs indicates that these modes may be responsible for the persisting self-correlation observed in the HFACs that subsequently caused the integrals to diverge. Additional calculations (not shown) also established that the same nondecaying modes, $k = 2\pi/40$ ucs from the 40 uc simulations, showed nondecaying behavior in the presence of other longer wavelength nondecaying modes, $k = 2\pi/80$ ucs in the 80 uc simulations. This observation ruled out the possibility that the phenomenon was only associated with the longest wavelength, lowest frequency modes in each simulation. The nondecaying behavior, however, could not be singly responsible for the divergent HFAC integrals, because it was observed in all cases where the domain length was longer than 40 ucs, regardless of whether or not the corresponding HFAC integral diverged. The actual conditions that lead to divergent HFAC integrals are likely to be quite complicated, because the system is highly nonlinear. Thus the exact cause of the divergence is not easily identifiable from the simulation data. Lepri, Livi, and Politi [2] have provided a possible explanation of this phenomenon in terms of hydrodynamic mode coupling. Their conclusions, however, are not necessarily transferable to our model because optical modes are present.

Regardless of whether or not nonattenuating modes actually exist in real PE chains, Fig. 4 shows that the TC

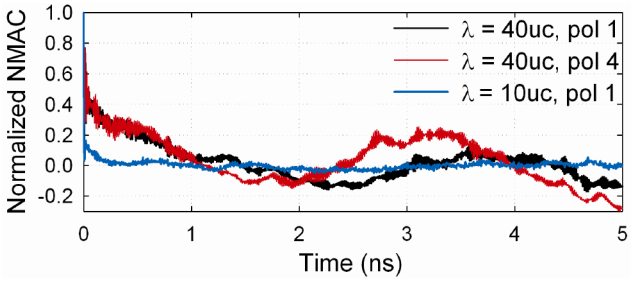

FIG. 3 (color online). NMAC functions for the transverse acoustic and torsional acoustic polarizations (1 and 4). NMACs from a 40 uc domain simulation, showing comparison of the $k = 2\pi/40$ uc modes which do not fully decay, with the $k = 2\pi/10$ uc mode from polarization 1, which exhibits typical decaying behavior.

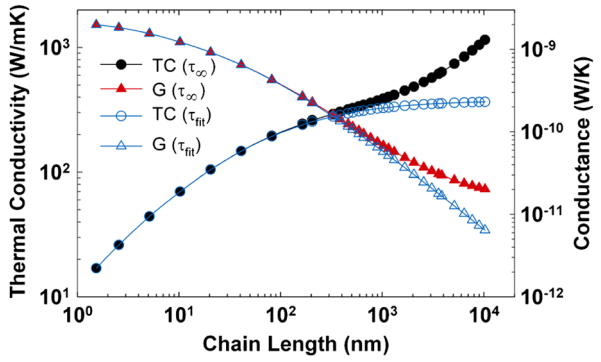

FIG. 4 (color online). Thermal conductivity (circles) and corresponding thermal conductance (triangles) predictions for a single PE chain. The τ_∞ curves assume that the (potentially nonattenuating) modes of polarizations 1 and 4, with wavelengths larger than 40 ucs, have infinite phonon-phonon relaxation times. The τ_{fit} curves use extrapolated values for the relaxation times of these modes.

of a single chain suspended between two contacts is several orders of magnitude higher than bulk PE. Here we have used the relaxation times obtained from a convergent 40 uc domain simulation and combined them with a boundary scattering term using Matthiessen's rule $1/\tau = 1/\tau_p + \upsilon/L$, such that the net relaxation time τ of each mode is affected by the phonon-phonon scattering rate within the chain $(1/\tau_p)$ as well as the boundaries between the chain and its thermal contacts. In Fig. 4, we have computed two sets of upper limiting values for the TC and its corresponding conductance G with respect to the chain length L. For both sets of predictions, the phonon-phonon relaxation times were linearly interpolated and extrapolated, as $k \rightarrow 0$, using a polynomial fit (approximately $\tau \propto 1/\nu$), from the NMAC data obtained in the 40 uc simulations. In the limiting case labeled τ_∞, however, we allowed any mode with a wavelength longer than 40 ucs in either polarization 1 or 4 to have an infinite relaxation time, which corresponds to the potentially nonattenuating modes previously discussed. Figure 4 shows that boundary scattering suppresses the effects of nonattenuating modes when the chain length is shorter than $\sim 1\ \mu$m. This is partly due to the fact that the largest TC contributions come from the longitudinal modes (labeled polarization 3 in Fig. 1), which have very high velocities $\sim 16\,000$ m/s. Beyond $1\ \mu$m, the τ_∞ limit increases indefinitely, while the τ_{fit} limit approaches a maximum ~ 350 W/m K, which agrees with our convergent Green-Kubo calculations. Inferring from Freeman, Morgan, and Cullen's results, their thermal conductivity (~ 55 W/m K) is lower than our prediction. One might expect their results to be higher than ours, because their use of the Kirkwood model did not consider the CH_2 internal degrees of freedom. However, Fig. 1 indicates that the Kirkwood model largely underestimates the acoustic mode group velocities, which have the strongest effect on the resultant thermal conductivity, as indicated by the BTE-TC expression.

The results in Fig. 4 suggest that the TC of single PE chains is several orders of magnitude larger than that of bulk PE and should increase with the chain length. Our relaxation time calculations lead to an estimate for the maximum conductance per chain, on the order of 10^{-9} W/K, which decreases with chain length. Although evidence of nonattenuating modes was observed, our calculations indicate that these modes will have a negligible effect, unless the chain is longer than $1\ \mu$m. With respect to the potential design of new materials that can exploit the transport properties of polymer chains, we anticipate that thermal contact resistance associated with the chain ends will be the most limiting factor. Recent experiments on the TC of PE chains have reported that the contact resistance is likely to dominate [20,21]. These reports neither confirm nor deny the claim that individual PE chains have high TC, but they do offer insight into the importance of contact resistance as a likely bottleneck. Nonetheless, it is our hope that these simulation results can stimulate interest in this area, as additional experiments are needed to determine the feasibility of using polymer chains as an ingredient for cheap thermally conducting materials.

We acknowledge funding from NSF Grant No. CBET-0755825 and computing resources provided by Intel.

[1] E. Fermi, J. Pasta, and S. Ulam, Los Alamos Report No. LA1940, 1955.
[2] S. Lepri, R. Livi, and A. Politi, Europhys. Lett. **43**, 271 (1998).
[3] S. Lepri, R. Livi, and A. Politi, Phys. Rep. **377**, 1 (2003).
[4] B. Li and J. Wang, Phys. Rev. Lett. **91**, 044301 (2003).
[5] J. J. Freeman, G. J. Morgan, and C. A. Cullen, Phys. Rev. B **35**, 7627 (1987).
[6] C. L. Choy *et al.*, J. Polym. Sci. B **37**, 3359 (1999).
[7] A. S. Henry and G. Chen, J. Comput. Theor. Nanosci. **5**, 141 (2008).
[8] A. J. C. Ladd, B. Moran, and W. G. Hoover, Phys. Rev. B **34**, 5058 (1986).
[9] A. McGaughey and M. Kaviany, Phys. Rev. B **69**, 094303 (2004).
[10] S. Plimpton, J. Comput. Phys. **117**, 1 (1995).
[11] J. Lukes and H. Zhong, J. Heat Transfer **129**, 705 (2007).
[12] S. Volz and G. Chen, Phys. Rev. B **61**, 2651 (2000).
[13] S. Stuart, A. B. Tutein, and J. A. Harrison, J. Chem. Phys. **112**, 6472 (2000).
[14] D. W. Brenner *et al.*, J. Phys. Condens. Matter **14**, 783 (2002).
[15] J. Che *et al.*, J. Chem. Phys. **113**, 6888 (2000).
[16] J. Kirkwood, J. Chem. Phys. **7**, 506 (1939).
[17] R. Hardy, Phys. Rev. **132**, 168 (1963).
[18] V. N. Popov, V. E. V. Doren, and M. Balkanski, Phys. Rev. B **61**, 3078 (2000).
[19] G. D. Barrera *et al.*, Macromolecules **39**, 2683 (2006).
[20] R. Y. Wang, R. A. Segalman, and A. Majumdar, Appl. Phys. Lett. **89**, 173113 (2006).
[21] Z. Wang *et al.*, Science **317**, 787 (2007).
[22] J.-S. Wang and B. Li, Phys. Rev. Lett. **92**, 074302 (2004).